U.S. DEPARTMENT OF COMMERCE
National Technical Information Service

PB-263 901

Dispersion of Roof-Top Emissions from Isolated Buildings. A Wind Tunnel Study

Environmental Sciences Research Lab, Research Triangle Park, NC

Prepared for

Northrop Services, Inc, Research Triangle Park, N C

Jan 77

PB 263 901

EPA-600/4-77-008
JANUARY 1977

Environmental Monitoring Series

REPRODUCED BY
NATIONAL TECHNICAL
INFORMATION SERVICE
U.S. DEPARTMENT OF COMMERCE
SPRINGFIELD, VA. 22161

RESEARCH REPORTING SERIES

Research reports of the Office of Research and Development, U.S. Environmental Protection Agency, have been grouped into five series. These five broad categories were established to facilitate further development and application of environmental technology. Elimination of traditional grouping was consciously planned to foster technology transfer and a maximum interface in related fields. The five series are:

1. Environmental Health Effects Research
2. Environmental Protection Technology
3. Ecological Research
4. Environmental Monitoring
5. Socioeconomic Environmental Studies

This report has been assigned to the ENVIRONMENTAL MONITORING series. This series describes research conducted to develop new or improved methods and instrumentation for the identification and quantification of environmental pollutants at the lowest conceivably significant concentrations. It also includes studies to determine the ambient concentrations of pollutants in the environment and/or the variance of pollutants as a function of time or meteorological factors.

This document is available to the public through the National Technical Information Service, Springfield, Virginia 22161.

EPA-600/4-77-006
January 1977

DISPERSION OF ROOF-TOP EMISSIONS FROM ISOLATED BUILDINGS

A Wind Tunnel Study

by

Roger S. Thompson
Meteorology and Assessment Division
Environmental Sciences Research Laboratory
Research Triangle Park, NC 27711

and

David J. Lombardi
Northrop Services Inc.
Research Triangle Park, NC 27711

ENVIRONMENTAL SCIENCES RESEARCH LABORATORY
OFFICE OF RESEARCH AND DEVELOPMENT
U.S. ENVIRONMENTAL PROTECTION AGENCY
RESEARCH TRIANGLE PARK, NORTH CAROLINA 27711

ia

DISCLAIMER

This report has been reviewed by the Environmental Sciences Research Laboratory, U.S. Environmental Protection Agency, and approved for publication. Mention of trade names or commercial products does not constitute endorsement or recommendation for use.

ABSTRACT

A fluid modeling study of the dispersion of roof-top emissions from rectangular buildings was performed in the meteorological wind tunnel of the EPA Fluid Modeling Facility. The basic building shape was a 0.18 meter cube. Variations included a building twice as wide and buildings twice and three times as high. Each building was placed in a 1.8 meter, simulated, neutral atmospheric boundary layer. Low momentum, non-buoyant emissions were released through an opening at the roof center. Photographs of flow visualization experiments are presented for a qualitative evaluation of the building wakes. Concentration measurements at ground level and aloft are presented for each case at downwind distances within 20 building heights. Concentrations are presented in a non-dimensional form for ease in application to full scale situations. The orientation of the wind to the building was found to significantly affect ground-level concentrations near the building. A 45° orientation of the cubical building increased the maximum ground-level concentration by a factor of six over that observed for a perpendicular orientation.

CONTENTS

Abstract iii

Figures vi

Symbols viii

1. Introduction 1

2. Conclusions 2

3. Experimental Techniques 3

4. Experimental Results 5

References 9

FIGURES

Number		Page
1	Top and side views of building model	11
2	Cubical model in wind tunnel test section during flow visualization experiment	12
3	Mean velocity profiles at location of cubical building without building in position (x=0) and downwind of building (x=2H,10H)	13
4	Local turbulence intensity at location of building without building in position (x=0) and downwind of the building (x=2H)	14
5	Flow visualization of Case 1	15
6	Vertical concentration profiles for Cases 1 and 8 (y=0)	16
7	Flow visualization of Case 1 (top view)	17
8	Lateral ground-level concentration profiles for Case 1	18
9	Ground-level concentrations for Cases 1, 2, 6, and 9 (y=0;z=0.025m)	19
10	Flow visualization of Case 2	20
11	Flow visualization of Case 2 (top view)	21
12	Vertical concentration profiles for Case 2 (y=0)	22
13	Lateral ground-level concentration profiles for Cases 1, 2, 3, 4, 6, and 9 (x=0.9m)	23
14	Vertical concentration profiles for Case 9 (y=0)	24
15	Ground-level concentrations for Cases 1, 3, 4, and 8 (y=0;z=0.025m)	25
16	Flow visualization of Case 3	26
17	Vertical concentration profiles for Case 3 (y=0)	27

TECHNICAL REPORT DATA
(Please read Instructions on the reverse before completing)

1. REPORT NO.	2.	3. RECIPIENT'S ACCESSION NO.
EPA-600/4-77-006		

4. TITLE AND SUBTITLE	5. REPORT DATE
DISPERSION OF ROOF-TOP EMISSIONS FROM ISOLATED BUILDINGS A Wind Tunnel Study	January 1977
	6. PERFORMING ORGANIZATION CODE
7. AUTHOR(S)	8. PERFORMING ORGANIZATION REPORT NO.
Roger S. Thompson, ESRL, EPA David J. Lombardi, Northrop Services, Inc.	Fluid Modeling Report No. 3
9. PERFORMING ORGANIZATION NAME AND ADDRESS	10. PROGRAM ELEMENT NO.
Environmental Sciences Research Laboratory Office of Research and Development U. S. Environmental Protection Agency Research Triangle Park, North Carolina 27711	1AA603
	11. CONTRACT/GRANT NO.
12. SPONSORING AGENCY NAME AND ADDRESS	13. TYPE OF REPORT AND PERIOD COVERED
Environmental Sciences Research Laboratory Office of Research and Development U. S. Environmental Protection Agency Research Triangle Park, North Carolina 27711	In-house
	14. SPONSORING AGENCY CODE EPA-600/09

15. SUPPLEMENTARY NOTES

16. ABSTRACT

A fluid modeling study of the dispersion of roof-top emissions from rectangular buildings was performed in the meteorological wind tunnel of the EPA Fluid Modeling Facility. The basic building shape was a 0.18 meter cube. Variations included a building twice as wide and buildings twice and three times as high. Each building was placed in a 1.8 meter, simulated, neutral atmospheric boundary layer. Low momentum, non-buoyant emissions were released through an opening at the roof center. Photographs of flow visualization experiments are presented for a qualitative evaluation of the building wakes. Concentration measurements at ground level and aloft are presented for each case at downwind distances within 20 building heights. Concentrations are presented in a non-dimensional form for ease in application to full scale situations. The orientation of the wind to the building was found to significantly affect ground-level concentrations near the building. A 45° orientation of the cubical building increased the maximum ground-level concentration by a factor of six over that observed for a perpendicular orientation.

17. KEY WORDS AND DOCUMENT ANALYSIS

a. DESCRIPTORS	b. IDENTIFIERS/OPEN ENDED TERMS	c. COSATI Field/Group
*Air pollution		13B
*Atmospheric diffusion		04A
Air flow		
*Boundary layer		20D
*Buildings		13M
*Environmental simulation		14B
wind tunnel		

18. DISTRIBUTION STATEMENT	19. SECURITY CLASS (This Report)	21. NO. OF PAGES
RELEASE TO PUBLIC	UNCLASSIFIED	46
	20. SECURITY CLASS (This page)	22. PRICE
	UNCLASSIFIED	

EPA Form 2220-1 (9-73)

FIGURES (Cont'd)

Number		Page
18	Flow visualization of Case 4	28
19	Vertical concentration profiles for Case 4 (y=0)	29
20	Flow visualization of Case 5	30
21	Flow visualization of Case 6	31
22	Flow visualization of Case 7	32
23	Vertical concentration profiles for Case 5 (y=0)	33
24	Vertical concentration profiles for Case 6 (y=0)	34
25	Vertical concentration profiles for Case 7 (y=0)	35

SYMBOLS

C	..Measured tracer concentration, % by vol.
C_{max}	..Maximum tracer concentration for a given profile, % by vol.
D	..Diameter of source, m
H	..Building height, m
L	..Building length, m
Q	..Source emission rate of tracer, % by vol. m^3/sec
Re	..Building Reynolds number, dimensionless
$U(z)$	..Mean wind speed at height z, m/sec
U_H	..Mean wind speed at building height in absence of building, m/sec
U_∞	..Mean free stream wind speed, m/sec
$\overline{u'^2}$	..Mean square of wind speed fluctuation, m^2/sec^2
W	..Building width, m
w	..Mean effluent speed at source, m/sec
x	..Coordinate in direction downwind from source, m
y	..Coordinate in crosswind direction, m
z	..Coordinate in vertical direction, m
α	..Exponent of wind speed profile, dimensionless
δ	..Boundary layer thickness, m
θ	..Angle between wind direction and normal to upwind building face, degrees
ν	..Kinematic viscosity of air, m^2/sec
ρ_s	..Density of effluent, Kg/m^3
ρ_a	..Density of ambient air, Kg/m^3
X	..Non-dimensional concentration coefficient

SECTION 1

INTRODUCTION

Because fluid modeling can accurately reflect the complex nature of turbulent air flow near structures, it is uniquely suited to the study of the dispersion of matter released from a building's roof-top. In such studies, two distinct phenomena have been observed downwind of an isolated, blunt structure. One is the development of an aerodynamic cavity of high turbulence and reverse flow caused by separation of the air flow over the building roof. The other is the confinement of roof-top emissions to the wake or dispersion envelope, which are determined by the shape of the building and by the approaching wind field.

The dispersion of roof-top emissions was modeled by Halitsky (1968) in a study of the concentration fields at and near rectangular buildings placed at various orientations to the wind. He used an approach flow of uniform mean velocity and low turbulence and an emission source located at the center of the roof. Although effluent momentum was varied, all emissions were non-buoyant. In another study, Yang and Meroney (1970) considered low momentum releases from all faces of a cubical structure and modeled both neutral and stratified boundary layers. Robins (1975) and Castro and Robins (1975) have performed fairly thorough studies of the turbulent wind field and plume dispersion in the vicinity of a surface mounted cube in a wind tunnel at Marchwood Engineering Laboratories, England. Conditions for some of their cases were quite similar to those used for the cubical building in the present study.

The present study, which was performed in the Environmental Protection Agency's Fluid Modeling Facility, extends previous work by analyzing concentration fields downwind of four different shapes of rectangular buildings. Block-shaped model buildings were placed in a simulated, neutral atmospheric boundary layer to determine the indluence of the wind field and building geometry on the dispersion of roof-top emissions. Only simple building shapes were used with no other buildings, trees, or hills located nearby. Air containing a low percentage of methane as a tracer was released from the center of the roof to model a low momentum, non-buoyant effluent. Ground-level and vertical concentration profiles were determined downwind by measuring tracer levels in samples taken at various positions.

SECTION 2

CONCLUSIONS

Smoke visualizations and measured concentration profiles are presented for generalized building shapes and wind directions. The situation was simplified in that the source was positioned at the roof center and the effluent was non-buoyant and had negligible momentum. Considering the cubical building model as the basis for comparision, some genral observations were made:

1) A change in the direction of the approaching wind significantly altered the shape and size of the aerodynamic cavity and the dispersion envelope. These changes resulted in different dispersion patterns and ground-level concentrations. A wind direction of 45° increased the maximum ground-level concentration by a factor of six. However, ground-level concentrations beyond x = 10H were essentially equal for the 0° and 45° cases.

2) Doubling the width of the building reduced by about 20 percent the concentrations below the building height (z = H) at a downwind distance of x = 5H. The ground-level maximum was approximately the same as that for the cube, but occurred nearer the building. Ground-level concentrations at distances beyond x = 5H were about 30 percent lower than for the cubical building.

3) Doubling the length of the building in the direction of the wind had little effect on the concentrations.

4) Doubling or tripling the height of the building elevated the plume and lowered the ground-level concentrations. The dispersion envelope over the building was similar for all three heights tested. Changing the wind direction from the perpendicular for the cases involving taller buildings increased the ground-level concentrations near the building.

The measurements of concentration as presented should be of use to numerical modelers in developing algorithms for predicting concentrations near pollution sources, such as roof-top incinerators, roof exhausts, etc. For full scale situations that are resonably similar to those of the block models of this study, the χ values of the figures can be applied directly to predict concentrations.

SECTION 3

EXPERIMENTAL TECHNIQUES

The experiment was performed in the EPA Meteorological Wind Tunnel (Snyder, 1974; Snyder et al., 1977). This low speed, open circuit wind tunnel has an 18 meter (m) long, 2.1 m high, 3.7 m wide test section in which atmospheric boundary layer air flow is simulated. Vortex generating fins as developed by Counihan (1969) were used to structure the desired boundary layer. The fins used for this study were 1.8 m high and produced a boundary layer height (δ) of 1.8 m. Two-dimensional roughness slats, 0.019 m high by 0.051 m wide and placed crosswind on 0.475 m centers, were mounted on the tunnel floor to maintain an equilibrium boundary layer over the length of the test section.

A dimensionless ratio of interest in modeling dispersion near buildings is the building Reynolds number, $Re = HU_H/\nu$; where H is the building height, U_H is the mean wind speed at $z = H$ with no building present, and ν is the kinematic viscosity of air. Ideally, the model Reynolds number and the full scale Reynolds number would be equal. However, in full scale situations, the Reynolds number is generally orders of magnitude larger than it is possible to obtain in the wind tunnel. Golden (1961) showed that concentration fields near building models are invariant with Reynolds number provided the building Reynolds number is greater than 11,000. In this study, the minimum Reynolds number for any case was 17,500.

For the model flow to be representative of atmospheric flows, the mean velocity field and the turbulence structure must be simulated. Profiles of mean velocity measured in a neutral atmosphere can be expressed as a power law of the form,

$$\frac{U(z)}{U_\infty} = \left(\frac{z}{\delta}\right)^\alpha$$

The value of the exponent, α, is governed by the roughness of the terrain. For a wind tunnel boundary layer flow, a power law with an exponent characteristic of the modeled terrain is desired. Similarly, components of local turbulence should be comparable to those in the atmospheric boundary layer.

Mean velocity and local turbulence intensity were measured with a hot-film anemometer. Vertical profiles were obtained where the building

would be located. The anemometer signal was digitized, linearized, and processed by a minicomputer. One minute averages at a sampling rate of 6000 samples per second were used.

Eight combinations of building shape and orientation to the wind were studied (Table 1 and Figure 1). The most extensive measurements were taken for Case 1, a cubical building (H=0.18 m) with a face perpendicular to the wind. An additional case, no. 8, was a repeat of case 1 with the mean wind speed twice that for case 1. It was performed as a check to verify that the dispersion in the building wake was independent of building Reynolds number. For all cases the model building was well within the boundary layer.

Flow visualization was used to gain insight into the qualitative features of the dispersion. An oil-fog generator was used to produce smoke which was released from the emission source. Sampling positions for quantitative measurements were based on observed plume trajectories. Figure 2 shows the cubical building model in position in the wind tunnel test section, the vortex generating fins, the floor roughness elements and scales to the right of the model. Marks on the scales are 0.05 m apart and the two scales were 0.9 m apart. Two tungsten lights were used to illuminate the smoke plume. Still photographs of each case were taken for a permanent record using a 35 mm camera with a 135 mm lens. The exposure of one second at f/16 was long enough to average most fluctuations of the plume.

For quantitative experiments, a 4.8 percent by volume mixture of methane-in-air was used as the tracer. The effluent rate, monitored through rotameters, was held at 4.0 liters per minute throughout the experiment. With the source diameter, D, of 0.0254 m, the effluent velocity was 0.13 m/s. Thus, the ratio of effluent velocity, w, to local velocity, U_H, was much less than 1.0 for all cases (see Table 1) as required for momentum effects to be neglible. Buoyancy due to the hydrocarbon tracer was also negligible; the ratio of effluent density to ambient density, ρ_s/ρ_a, was 0.98 for all cases.

Samples were drawn through a 0.002 m diameter sampling probe and passed through a flame ionization detector to determine tracer concentrations. The ambient hydrocarbon background was measured before and after each run. Since the background variation was small, it was assumed to be linear with time to compute values to correct the raw data. The output of the flame ionization detector was digitized and processed on a minicomputer. One minute averages at a sampling rate of 2000 samples per second were used.

SECTION 4

EXPERIMENTAL RESULTS

Velocity and turbulence measurements were made to evaluate how well the model flow represented the atmospheric boundary layer. Measurements were also made at several positions in the field downwind of the building. The mean freestream speed was equal to 2 m/s (except for Case 8).

Profiles of the mean velocity measured over the release point with the building removed and at two locations downwind of the building are shown in Figure 3. The mean velocity profile in the approach to the building (x=0) is handily approximated by a one-seventh power law. In the far-wake region of the cubical building (x=10H) the velocity profile has nearly recovered to the approach profile. A one-seventh power law profile is typical of flow over flat rural topography with low shrubbery (Davenport, 1963). Although hot-film anemometer measurements are unreliable near the building where turbulence levels are high and flow reversals occur, severe distortion of the mean velocity profile caused by the building is observed in the profile at x=2H.

Longitudinal turbulence intensities of the approach flow were also comparable to field observations made in a neutral atmosphere. The maximum local turbulence intensity in the approach flow, $\sqrt{u'^2}/U = 0.24$, occurred at ground level and the intensity subsequently decreased with height to wind tunnel back-ground turbulence levels. Approach flow turbulence (x = 0), shown in Figure 4, was not unlike the field data of Harris (1968) in tendency and magnitude. A previous study (Huber and Snyder, 1976) using this same boundary layer examined dispersion from short stacks. Analysis of the lateral and vertical spreading of the plume from an isolated stack in that study showed the dispersion to be represented by Pasquill-Gifford category "C", slightly unstable, for a model scale on the order of 1:100. In the wake of the cubical building (x = 2H), the local turbulence intensity measurements were unreliable but showed the profile to be erratic and the turbulence to be of large magnitude. However, the presence of the building did not seem to disturb the flow above approximately the 1.5H level for this approach flow.

As was to be expected, the flow separated at the leading edge of the top of the building model for the perpendicular orientation. A cavity of highly turbulent and reversing flow formed over the building and extended to the lee of the building. Some features of the circulation in this cavity can be seen by analysis of the flow visualization photographs, but an appreciation for the complex turbulent nature of the flow in this region requires first hand observation.

Castro and Robins (1975) reported on the dependence of the characteristics of the cavity on the thickness of the approach flow boundary layer. Their surface pressure and velocity measurements indicated that the flow reattached on a cubical building roof at x = -0.25H, for the type of boundary layer used in the present study. Observations of the dispersing smoke in the present study did not substantiate their claim. The time-averaged photographs are similar to those of Yang and Meroney (1970) that did not show a reattached flow.

Smoke visualization studies provide insight into gross features of the dispersion of contaminants but should not be used to make detailed inferences. When photographed, lighting and exposure differences can make the same situation appear quite differently. Hence, concentration measurements of a tracer released from the source must be relied upon for the quantitative evaluation and comparison of dispersion.

All measured concentrations, C, were made non-dimensional with the source emission rate, Q, according to the corresponding building height, H, and mean wind speed at that height, U_H;

$$\chi = CU_H H^2/Q.$$

This should be kept in mind when comparing values for different building heights. To avoid interference with the surface roughness slats, a height of z = 0.025 m was taken as "ground-level" for concentration measurements. Coordinates (x, y, z) are defined in Figure 1.

Of the building shapes considered, a cubical building is the most elementary. Figure 5 demonstrates the behavior of a roof centered release from a cubical model when the wind is perpendicular to a side (Case 1). Reverse flow just above the top of the cube advected some of the effluent to the upwind edge of the roof. The height of the dispersion envelope determined from the smoke visualization was approximately 1.5H over the building and approximately 2.0H at a downwind distance of 5H. Vertical concentration profiles (Figure 6) indicate similar envelope heights. The maximum concentration for the vertical profile at a downwind distance of x = 2H occurred at an elevation of z = H. At distances farther downwind, the peak value indicated by each profile moved closer to the ground. The lateral spread of the plume can be observed to be only slightly greater than the building width in the top view of the visualization (Figure 7). Measured concentrations at x = 2H and x = 5H show the plume width (plume edge taken as point where $C = 0.1C_{max}$) to be approximately 2.5H and 3.5H, respectively (Figure 8).

A longitudinal, ground-level profile along the plume centerline (Figure 9) indicated a maximum ground-level concentration of $\chi = 0.43$ at a distance of x = 5H. Robins (1975) reports values for a case similar to Case 1. His results, converted to the scaling used here, show a maximum ground-level

concentration $\chi = 0.31$ to occur at a distance of $x = 3H$. The exit momentum ratio for his model was 6 times that used here and his velocity ratio U_H/U_∞ was lower than in this study.

A different wind direction produces a significant change in the way the roof-top emissions disperse. When a corner of the cube was pointed into the wind (Case 2, Figure 10), flow reversals atop the building did not occur as in Case 1. Emissions were swept directly over the downwind building corner with no reverse flow over the building roof (Figure 11) and more smoke reached ground-level immediately downwind of the building than was observed for Case 1. With this building orientation, the dispersion envelope did not extend far above the building, nor did it grow rapidly with increasing downwind distance. The vertical concentration profiles illustrate the differing characteristics (See Figure 6 and 12). Maximum concentrations for each profile occurred at ground-level for distances greater than $x = 5H$. However, for the profile at $x = 2H$, the maximum concentration occurred at an elevation of approximately $z = 0.66H$. The smoke envelope was wider for Case 2 than for Case 1 (at $x = H$, the observed width was 1.5H for Case 1 and 2H for Case 2). This is in part due to the increased projected area of the building into the wind. The flow separated at the corners of the building (Figure 11) to produce standing vortices which also increased the width of the dispersion envelope. Ground-level concentrations were much higher for Case 2 than for Case 1 up to about $x = 5H$ but they were nearly equal by $x = 10H$ (Figure 9).

For cases where cubical buildings are oriented at other angles to the mean flow, emissions may be expected to produce concentration levels that are between those of Case 1 and Case 2. Case 9 was such a configuration with the building rotated to an angle $\theta = 22.5°$. The plume for this case was found to be slightly skewed about the line $y = 0$ (Figure 13). The longitudinal concentration profile (Figure 9) and the vertical profiles (Figure 14) were measured directly downwind of the release point. In Figure 9 one can see that near the building the concentration levels for case 9 fell between those of Cases 1 and 2. Farther downwind, concentrations for all three cases approached the same levels. The vertical profiles of Case 9 (Figure 14) were similar to those of Case 2 beyond $x = 5H$.

Case 8 was a repeat of Case 1 at twice the freestream velocity. It was performed as a check on the Reynolds number independence of the dispersion. A longitudinal, ground-level concentration profile (Figure 15) and a vertical profile at $x = 5H$ (Figure 6) are practically identical to the corresponding profiles for Case 1. The close agreement of these profiles indicates that the dispersion field did not change substantially with a doubling of the building Reynolds number.

A block with its width, W, twice the other dimensions (Case 3), produced an envelope of somewhat greater vertical extent (Figure 16) than for Case 1. For Case 3 the vertical concentration profiles (Figure 17) had shapes similar

to those for Case 1. However, concentrations below the building height (z=H) were lower by approximately 20 percent. This effect can be attributed to more lateral and vertical spreading of the plume. The ground-level concentrations along the plume centerline (Figure 15) were lower by about 30 percent at locations far from the building (x > 5H). The maximum ground-level value was about the same as for Case 1, but it occurred closer to the building.

Case 4, a model building with its length in the direction of the wind twice the other dimensions, had a similar vertical bound on the envelope (Figure 18). The vertical profiles for Case 4 (Figure 19) were also similar to those for Case 1. Concentrations near the plume centerline for the x = 2H profile were only slightly higher for Case 4. The ground-level concentrations along the plume centerline were only slightly lower than the Case 1 (Figure 15).

The building that was twice as high as its other dimensions, Case 5, had an envelope directly over the building (Figure 20) which was similar to that of Case 1; but its height did not increase downwind of the building. Also illustrated by Figure 20 is that little of the smoke reached the ground immediately downwind of the building. With this building rotated 45° (Case 6, Figure 21), however, a considerable amount of the smoke reached the ground. The flow observed over the building roof for Case 6 was similar to that for Case 2. The emissions were swept directly over the downwind corner of the roof into the cavity of reverse flow.

Case 7 (Figure 22), involved the use of a building three times as high as the building used in Case 1, and had about the same growth in vertical bound as Case 5. Essentially no smoke reached the ground near the building. Near building, ground-level concentrations for Cases 5 and 7 were not high enough above background to obtain reliable measurements. This was in agreement with the smoke visualization photographs.

Vertical profiles for Cases 5 and 6 are shown in Figures 23 and 24. With this taller building rotated 45°, concentrations aloft at x = H were roughly three times those that occurred with the building perpendicular to the wind. The vertical profile flattens out so that the maximum occurs at the ground level near x = 2H for Case 6 but not until after x = 4H for Case 5. The vertical profiles for Case 7 (Figure 25) were similar to those for Case 5.

REFERENCES

Castro, I. P. and A. G. Robins (1975): The Effect of a Thick Incident Boundary Layer on the Flow Around a Small Surface Mounted Cube. Marchwood Engineering Laboratories Report R/M/N795, Central Electricity Generating Board, England.

Counihan, J. (1969): An Improved Method of Simulating an Atmospheric Boundary Layer in a Wind Tunnel. Atm. Env. 3, p. 197-214.

Davenport, A. G. (1963): The Relationship of Wind Structure to Wind Loading. Paper 2, Proc. of Conf. on "Wind Effects on Buildings and Structures", (Nat. Phys. Lab., Teddington, Middlesex, June 1963) HMSO, London, 1965, p. 54-102.

Golden, J. (1961): Scale Model Techniques. M. S. Thesis, College of Engr., NYU, May.

Halitsky, J. (1968): Gas Diffusion Near Buildings, in Meteorology and Atomic Energy, 1968, edited by David H. Slade, p. 221-255.

Harris, R. I. (1968): Measurement of Wind Structure at Heights up to 598 ft. above Ground-Level, Symp. Wind Effects on Buildings and Structures, Loughborough Univ. Tech. (Dept. of Transport Technology).

Huber, A. H. and W. H. Snyder (1976): Building Wake Effects on Short Stack Effluents. Preprint Volume of the American Meteorological Society 3rd Symposium on Atmospheric Turbulence, Diffusion and Air Quality. Raleigh, NC, October 19-20, 1976.

Robins, A. G. (1975): Plume Dispersion in the Vicinity of a Surface Mounted Cube. Marchwood Engineering Laboratories Report R/M/R220, Central Electricity Generating Board, England.

Snyder, W. H. (1974): Fluid Modeling Program of the Meteorology Laboratory, U.S. Environmental Protection Agency. Chapter 31 of Proceedings of the Fifth Meeting of the Expert Panel on Air Pollution Modeling. NATO-CCMS, N. 35.

Snyder, W. H., R. S. Thompson, and R. E. Lawson, Jr. (1977): The EPA Meteorological Wind Tunnel: Design, Construction, and Operating Details. Environmental Protection Agency, Research Triangle Park, NC (In preparation).

Yang, B. T. and R. N. Meroney (1970): Gaseous Dispersion Into Stratified Building Wakes. FDDL Technical Report, CSU, CER70-71BTY RNM-8.

Table 1. GEOMETRY AND DEFINING PARAMETERS FOR EACH CASE

	Shape, m[a]			Parameter[b]				
Case	L	W	H	θ, degrees	H/δ	U_H, m/sec	w/U_H	$Re=\frac{U_H H}{\nu}$
1	0.18	0.18	0.18	0	0.1	1.46	0.090	17,500
2	0.18	0.18	0.18	45	0.1	1.46	0.090	17,500
3	0.18	0.36	0.18	0	0.1	1.46	0.090	17,500
4	0.36	0.18	0.18	0	0.1	1.46	0.090	17,500
5	0.18	0.18	0.36	0	0.2	1.62	0.081	38,900
6	0.18	0.18	0.36	45	0.2	1.62	0.081	38,900
7	0.18	0.18	0.54	0	0.3	1.70	0.078	61,000
8	0.18	0.18	0.18	0	0.1	2.92	0.045	35,000
9	0.18	0.18	0.18	22.5	0.1	1.46	0.090	17,500

a L = length, W = width, H = height.

b θ = building orientation to wind, H/δ = ratio of building height to boundary layer height, U_H = mean wind speed at building height, w/U_H = ratio of effluent velocity to local velocity, Re = Reynolds number.

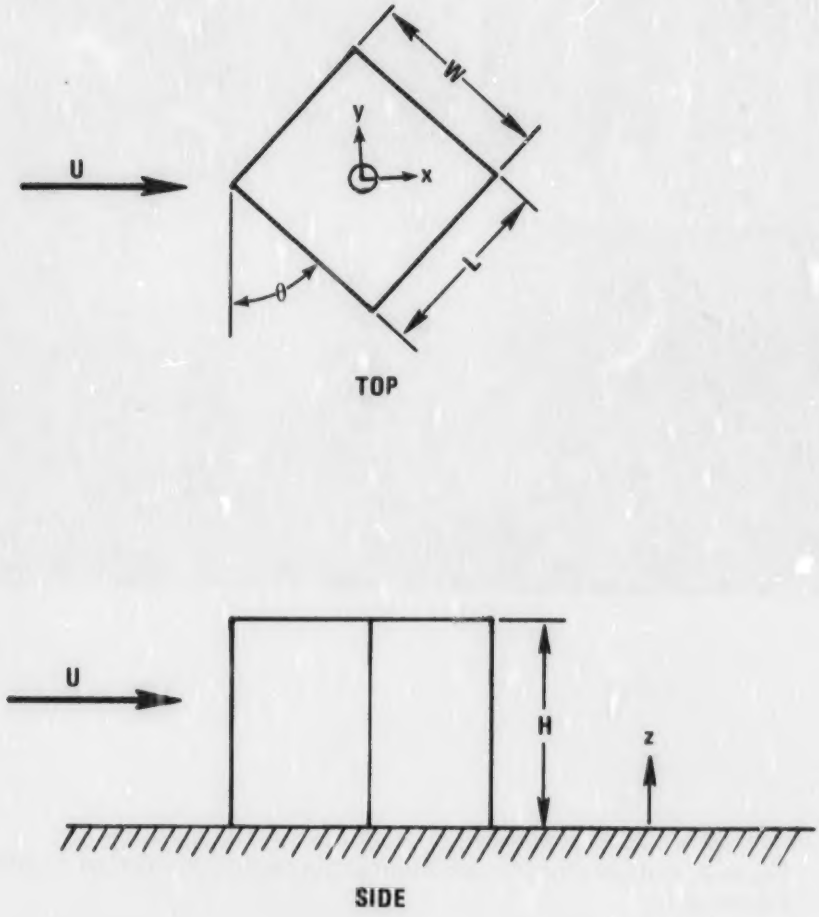

Figure 1. Top and side views of building model.

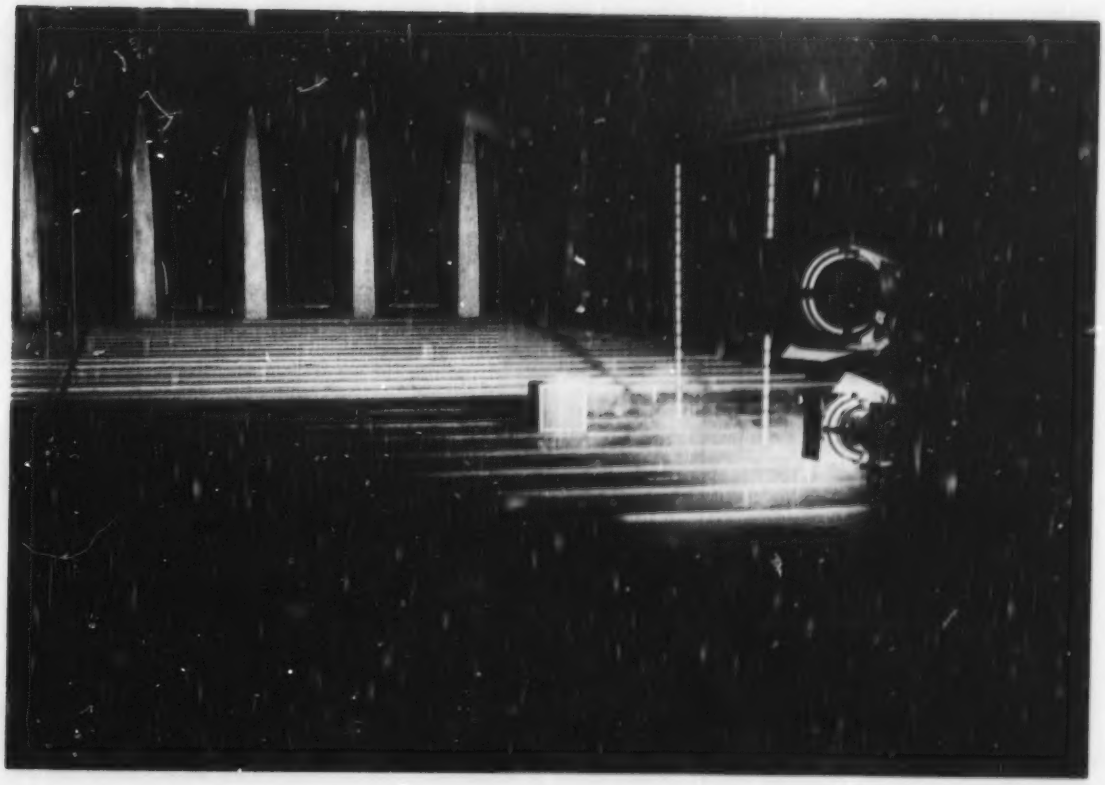

Figure 2. Cubical model in wind tunnel test section during flow visualization experiment.

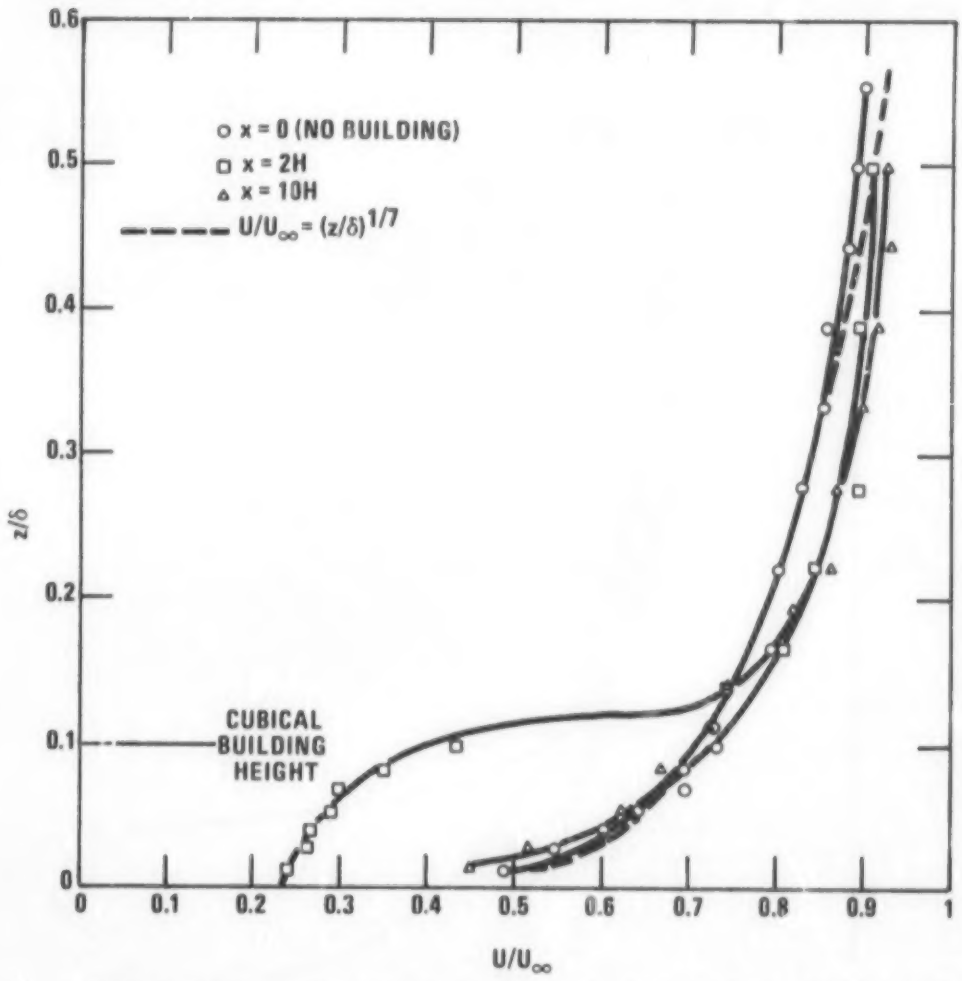

Figure 3. Mean velocity profiles at location of cubical building without building in position (x=0) and downwind of building (x=2H, 10 H).

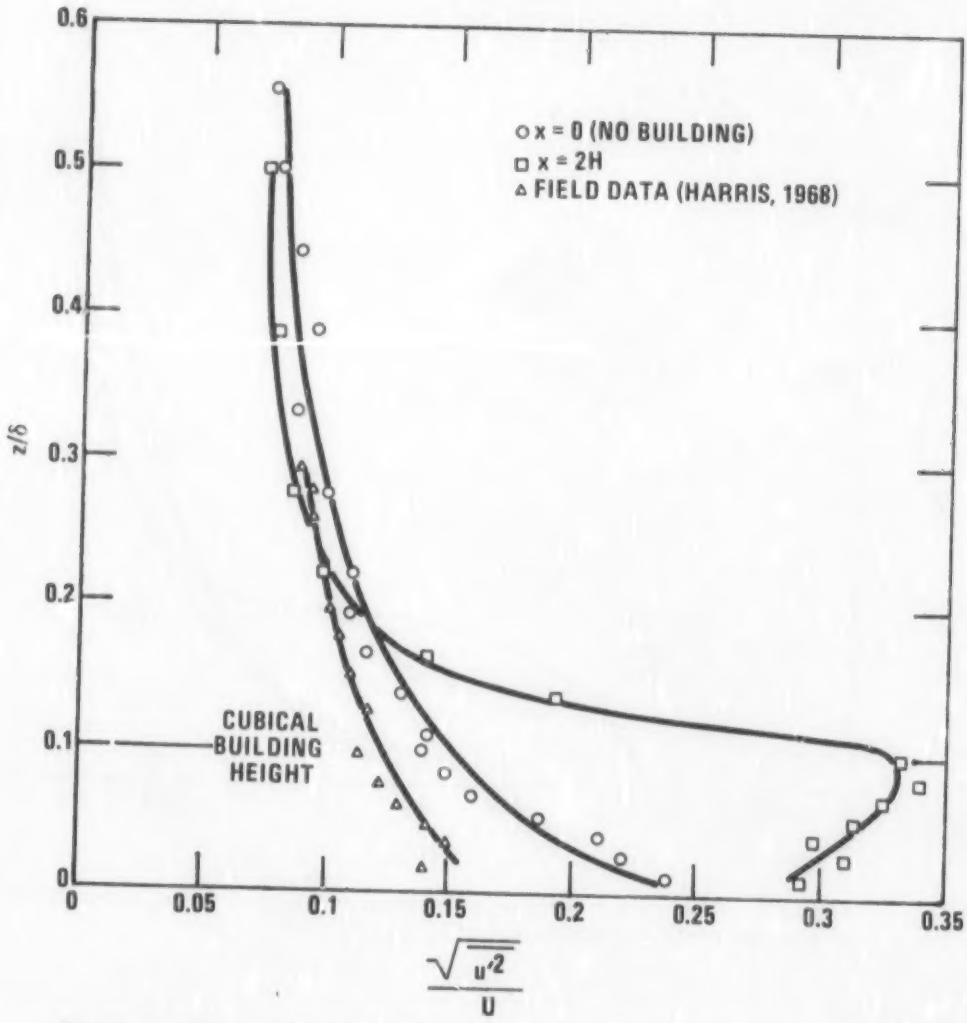

Figure 4. Local turbulence intensity at location of cubical building without building in position (x=0) and downwind of the building (x=2H).

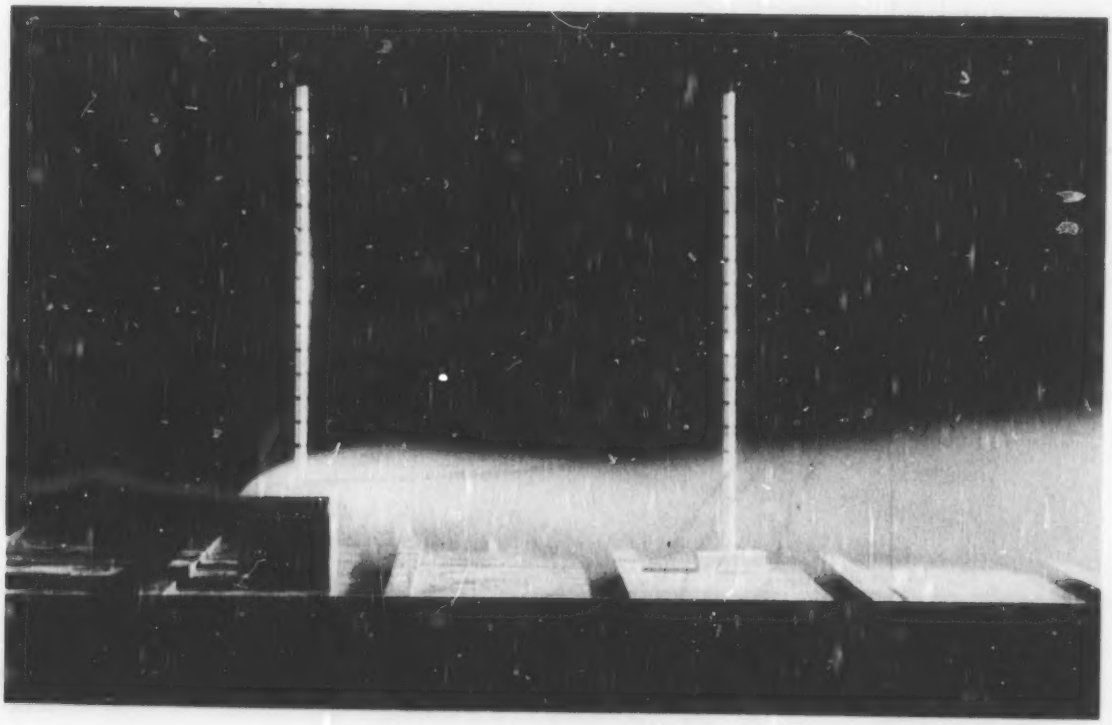

Figure 5. Flow visualization of Case 1.

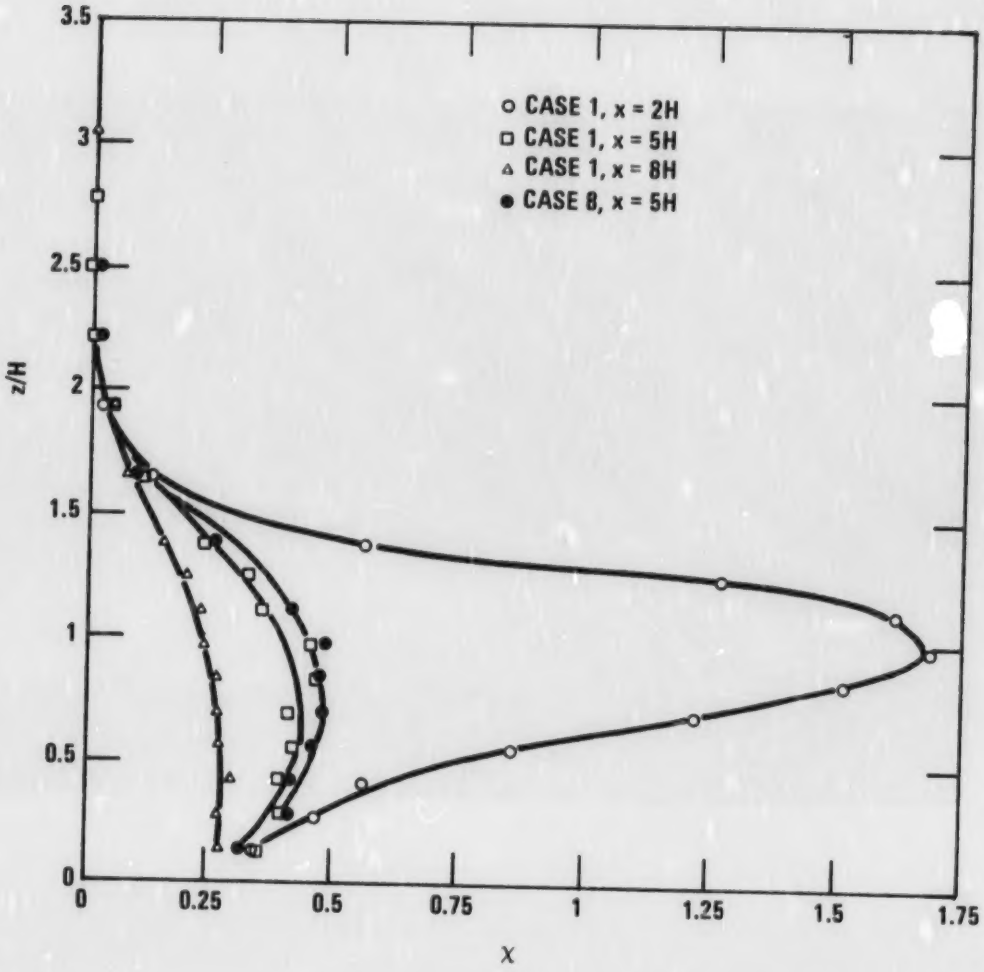

Figure 6. Vertical concentration profiles for Cases 1 and 8. (y = 0.)

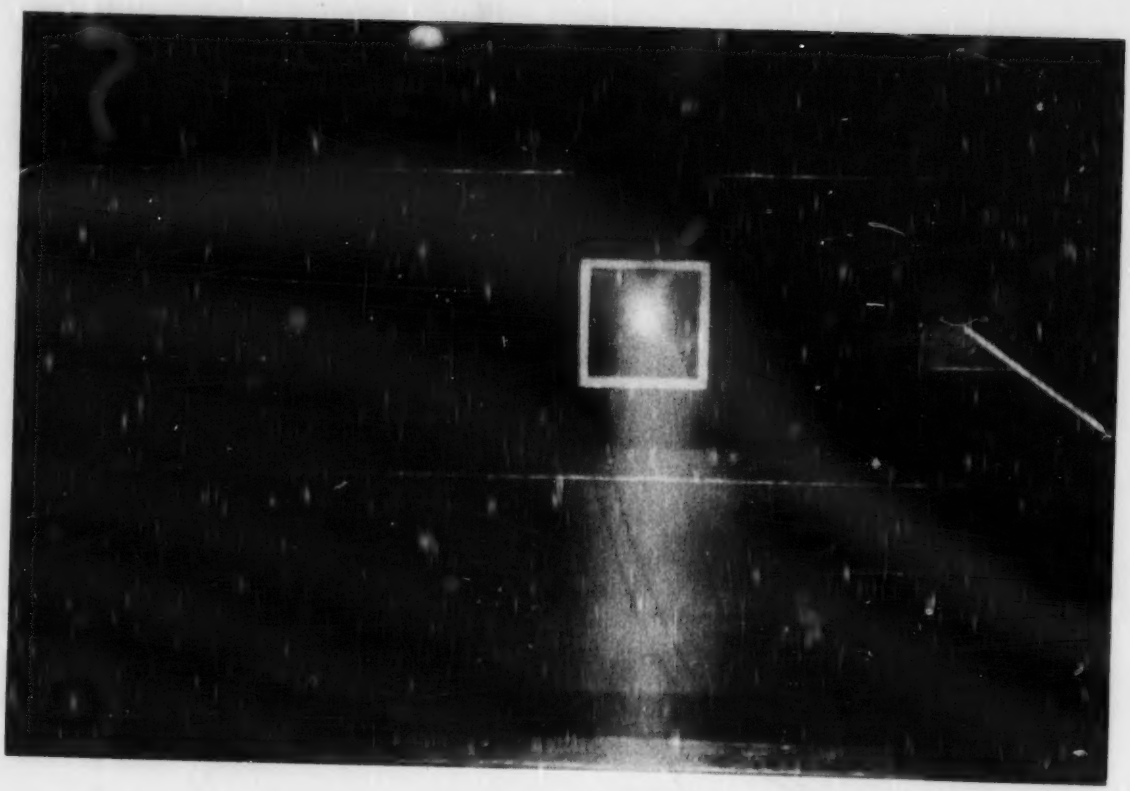

Figure 7. Flow visualization of Case 1 (top view).

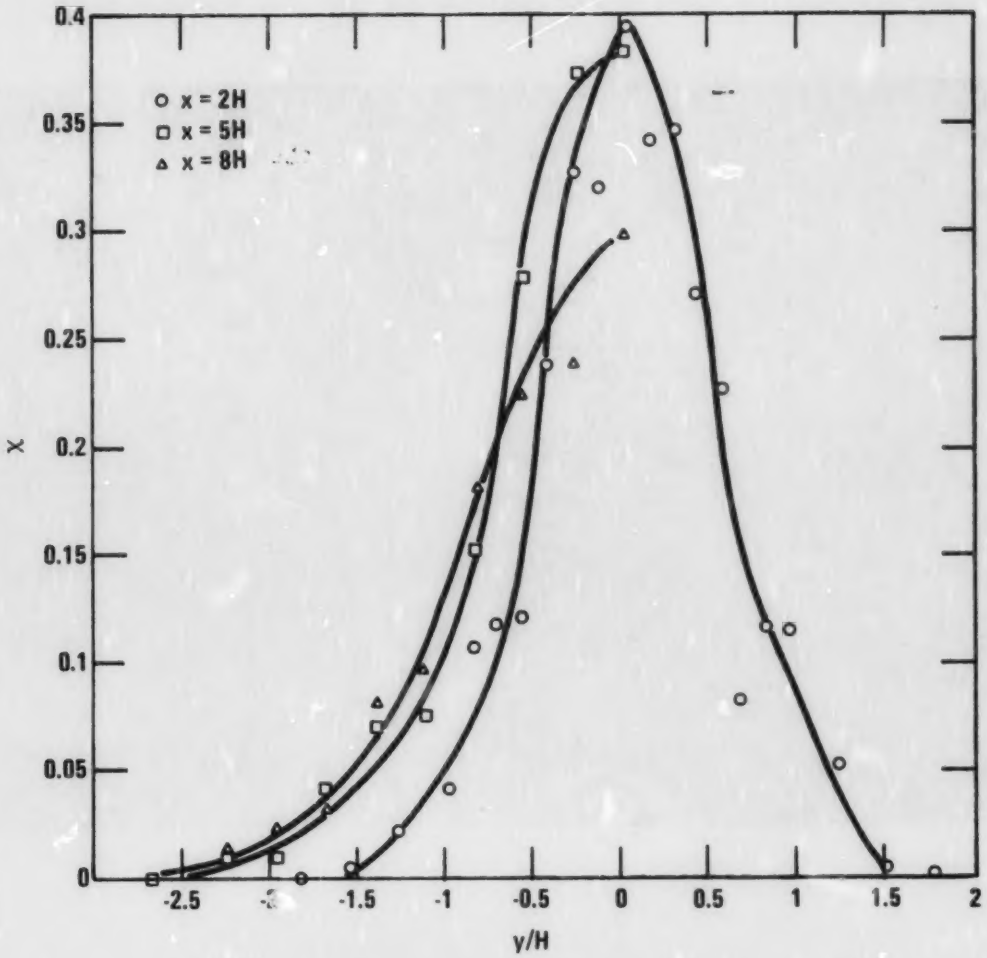

Figure 8. Lateral ground-level concentration profiles for Case 1.

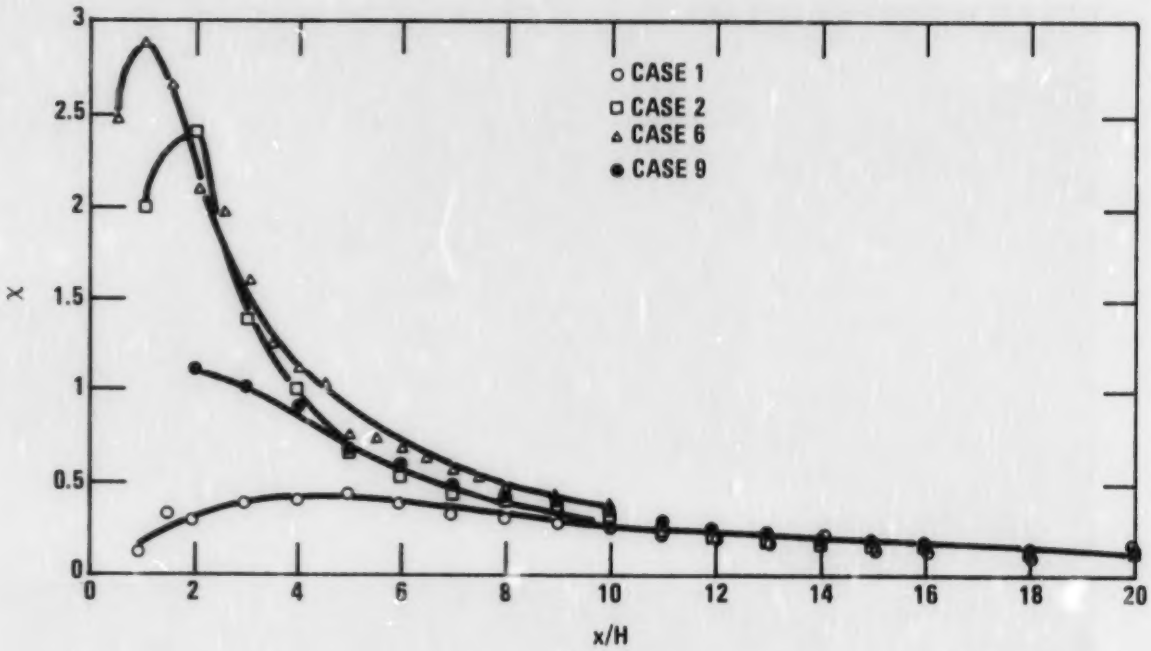

Figure 9. Ground-level concentrations for Cases 1, 2, 6, and 9. (y = 0; z = 0.025 m.)

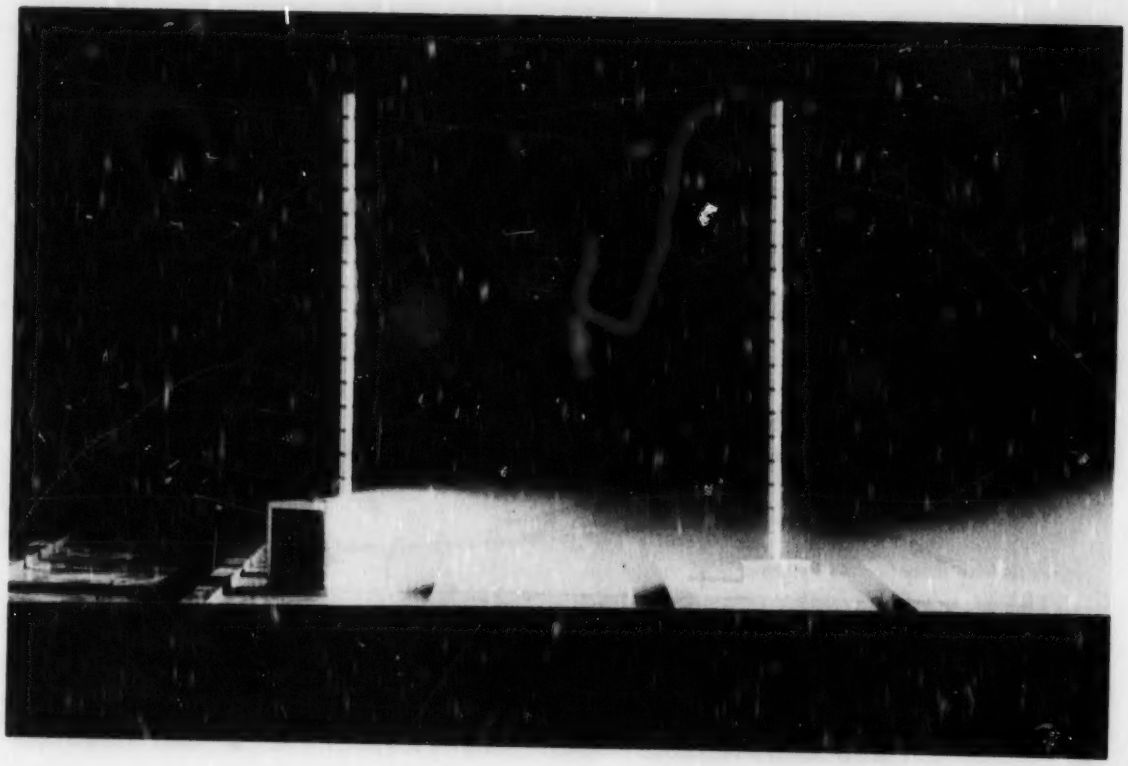

Figure 10. Flow visualization of Case 2.

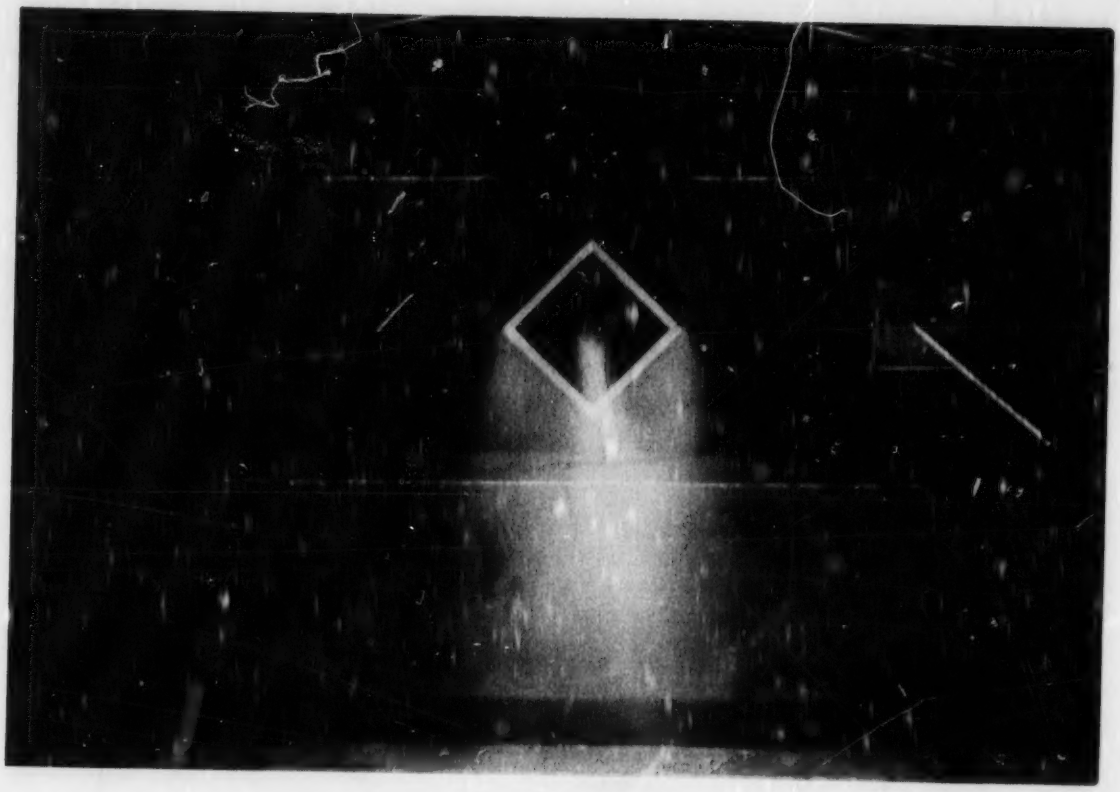

Figure 11. Flow visualization of Case 2 (top view).

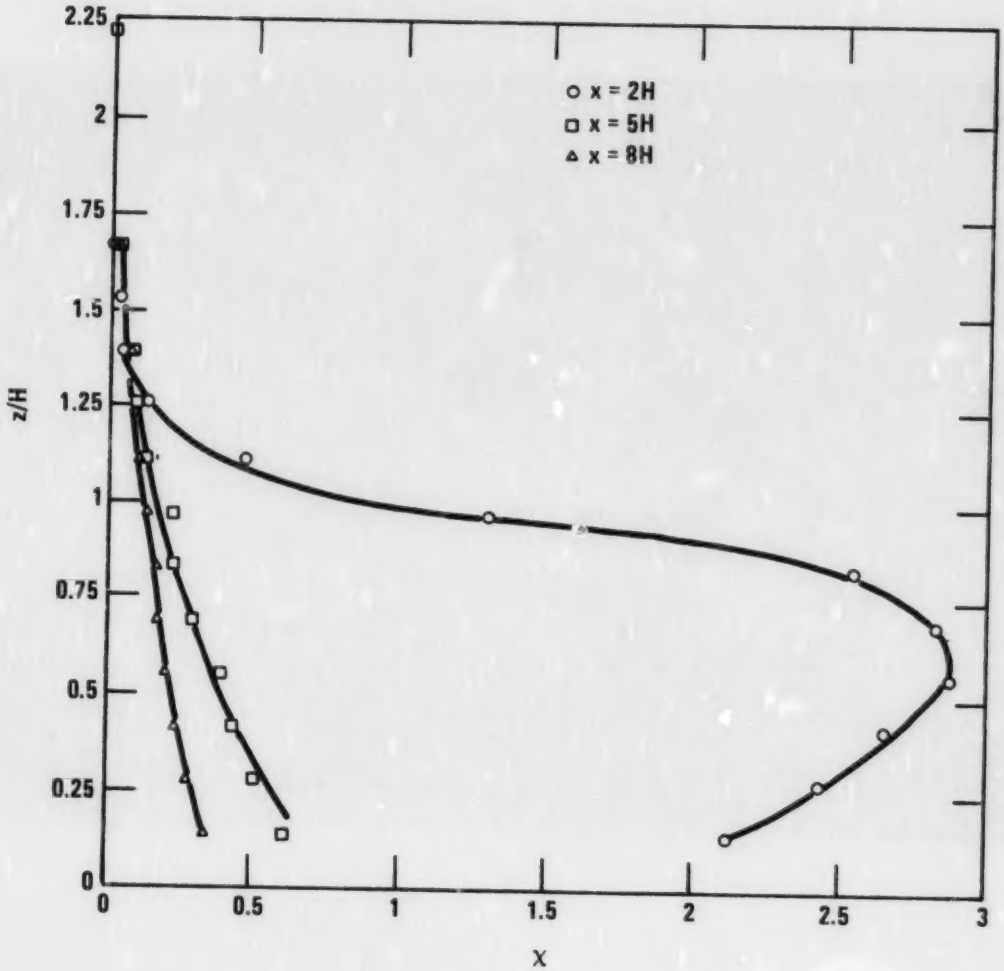

Figure 12. Vertical concentration profiles for Case 2. (y = 0.)

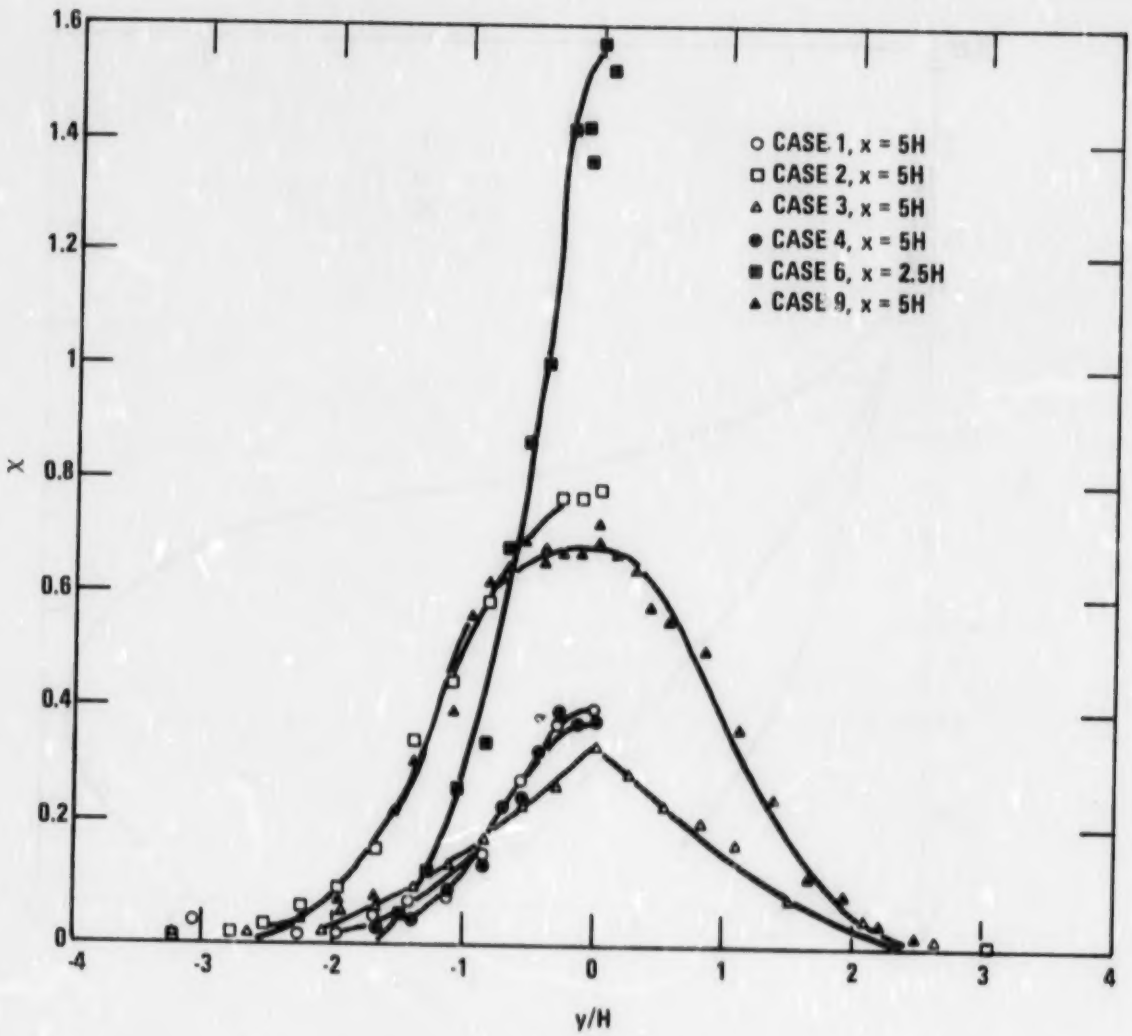

Figure 13. Lateral ground-level concentration profiles for Cases 1, 2, 3, 4, 6, and 9. (x = 0.9 m.)

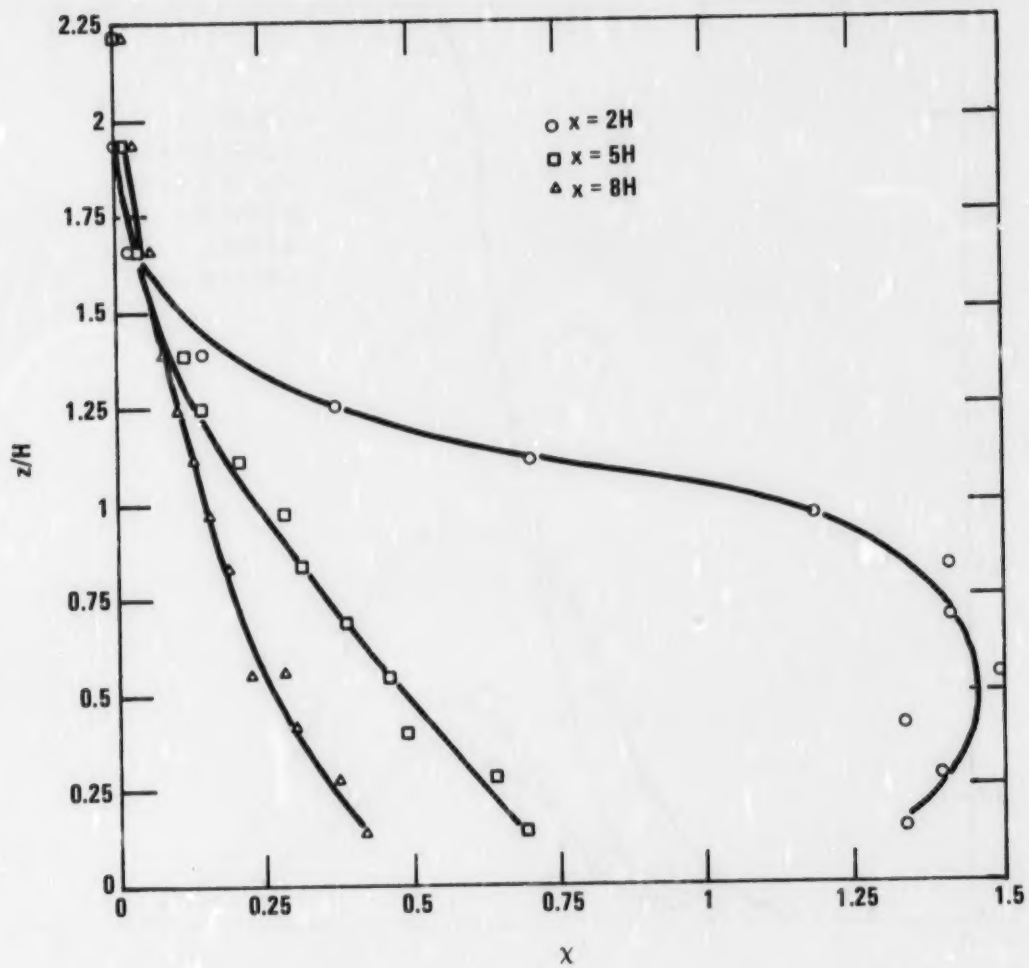

Figure 14. Vertical concentration profiles for Case 9. (y = 0.)

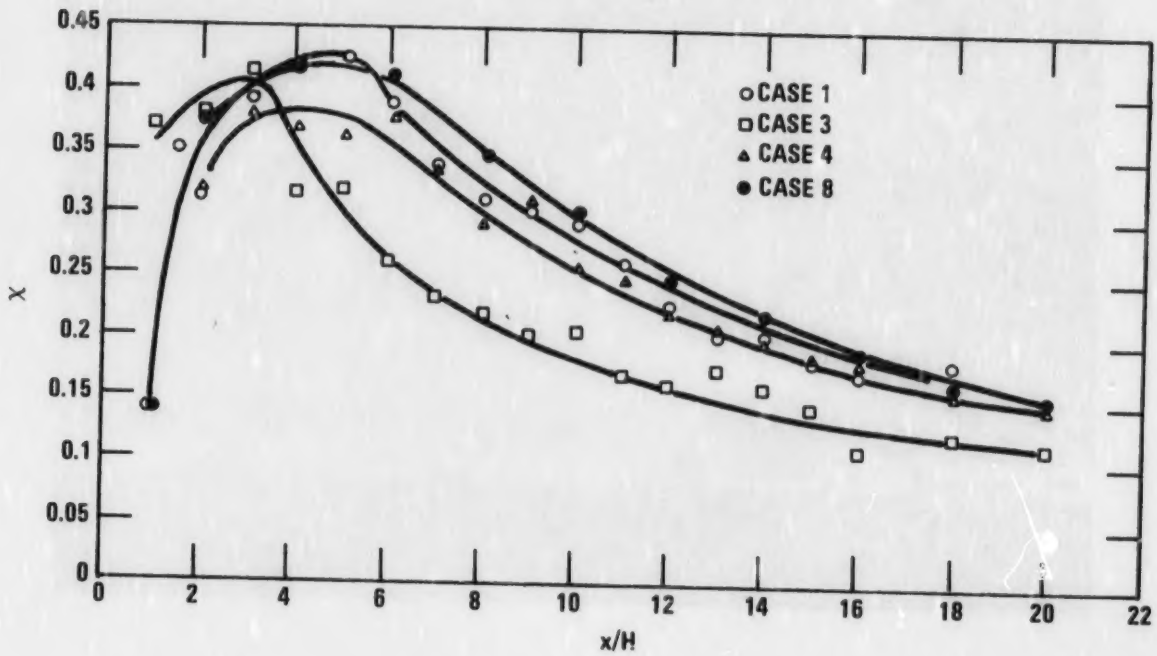

Figure 15. Ground-level concentrations for Cases 1, 3, 4, and 8. (y = 0; z = 0.025 m.)

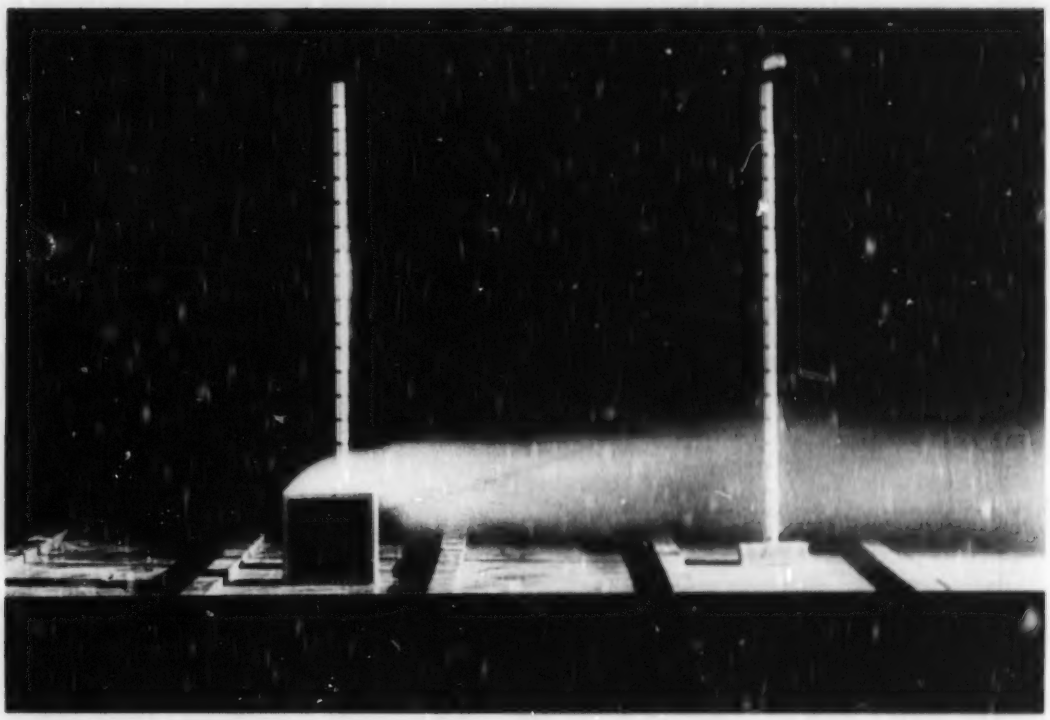

Figure 16. Flow visualization of Case 3.

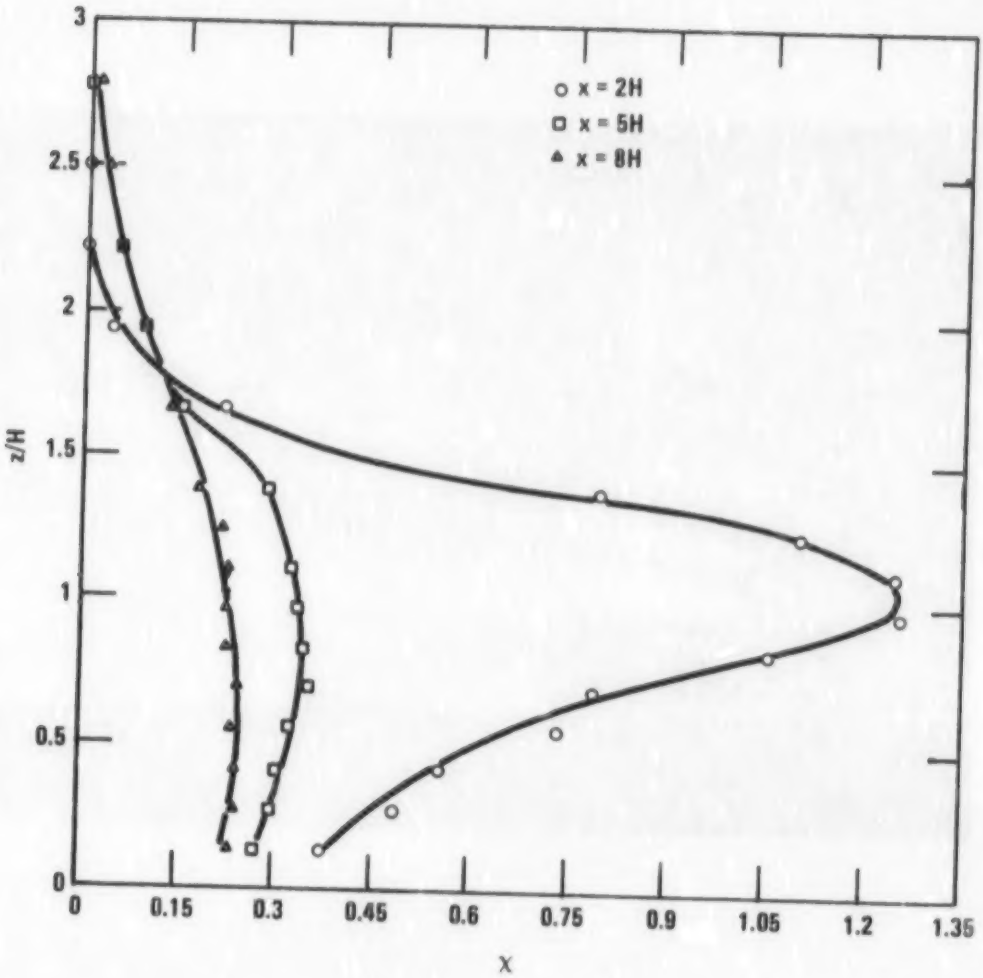

Figure 17. Vertical concentration profiles for Case 3. (y = 0.)

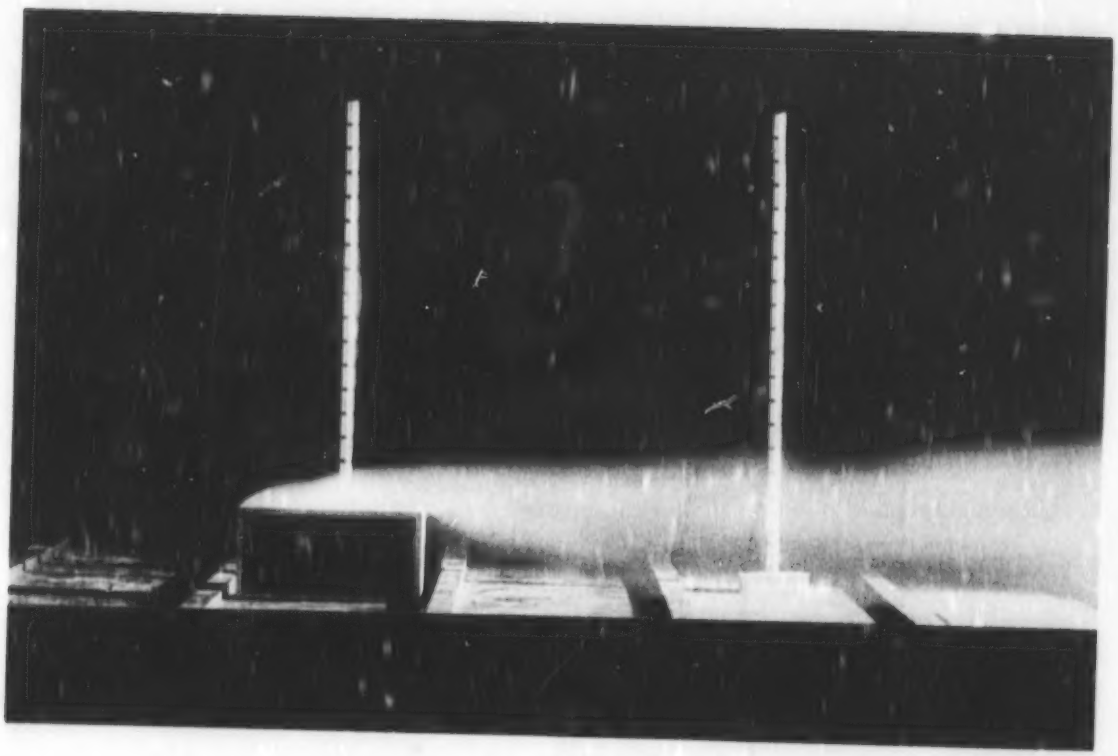

Figure 18. Flow visualization of Case 4.

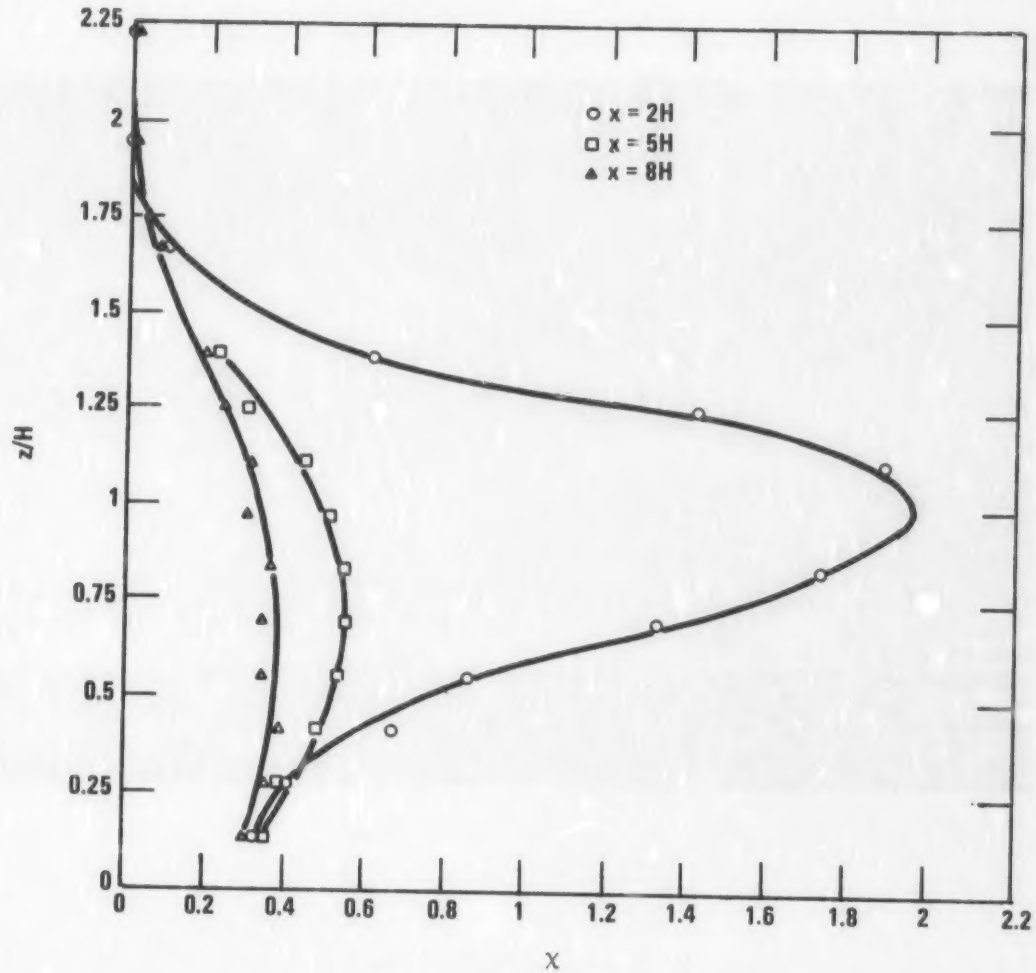

Figure 19. Vertical concentration profiles for Case 4. (y = 0.)

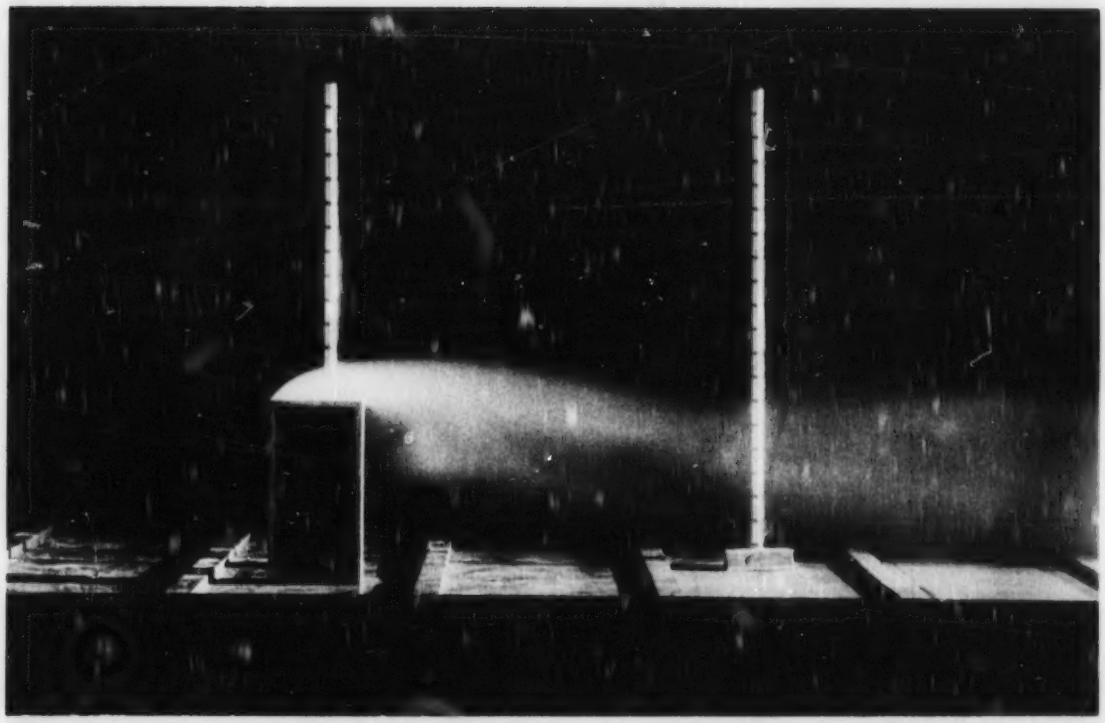

Figure 20. Flow visualization of Case 5.

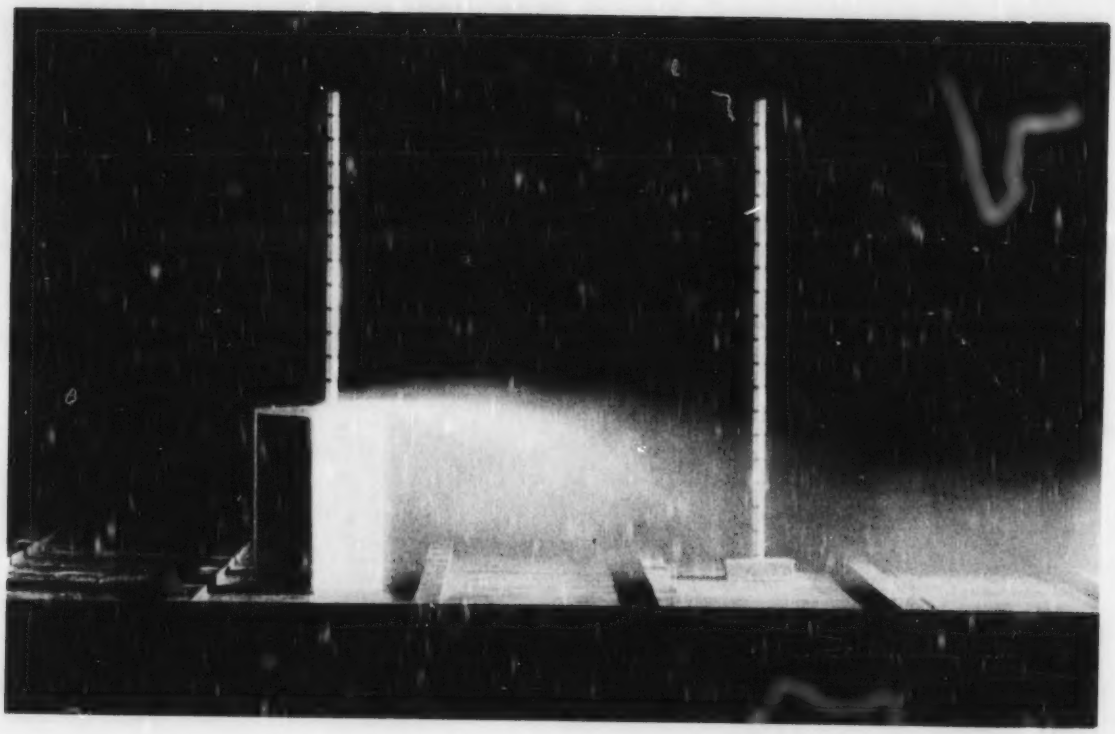

Figure 21. Flow visualization of Case 6.

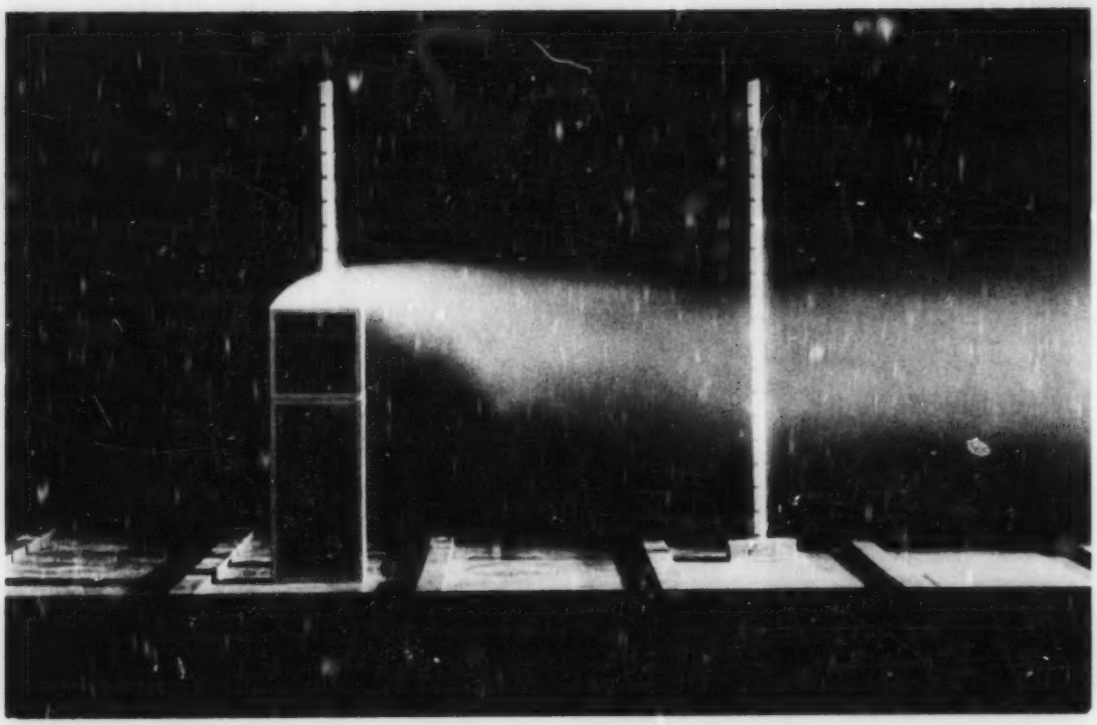

Figure 22. Flow visualization of Case 7.

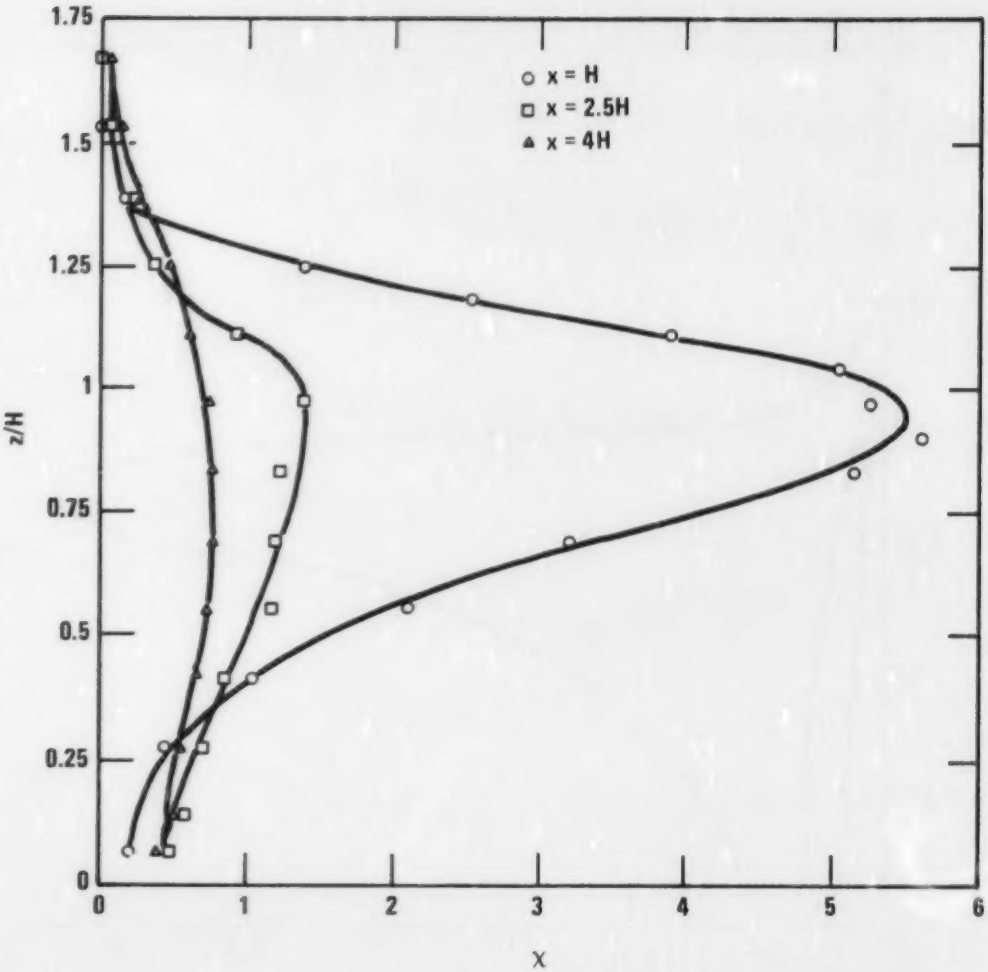

Figure 23. Vertical concentration profiles for Case 5. (y = 0.)

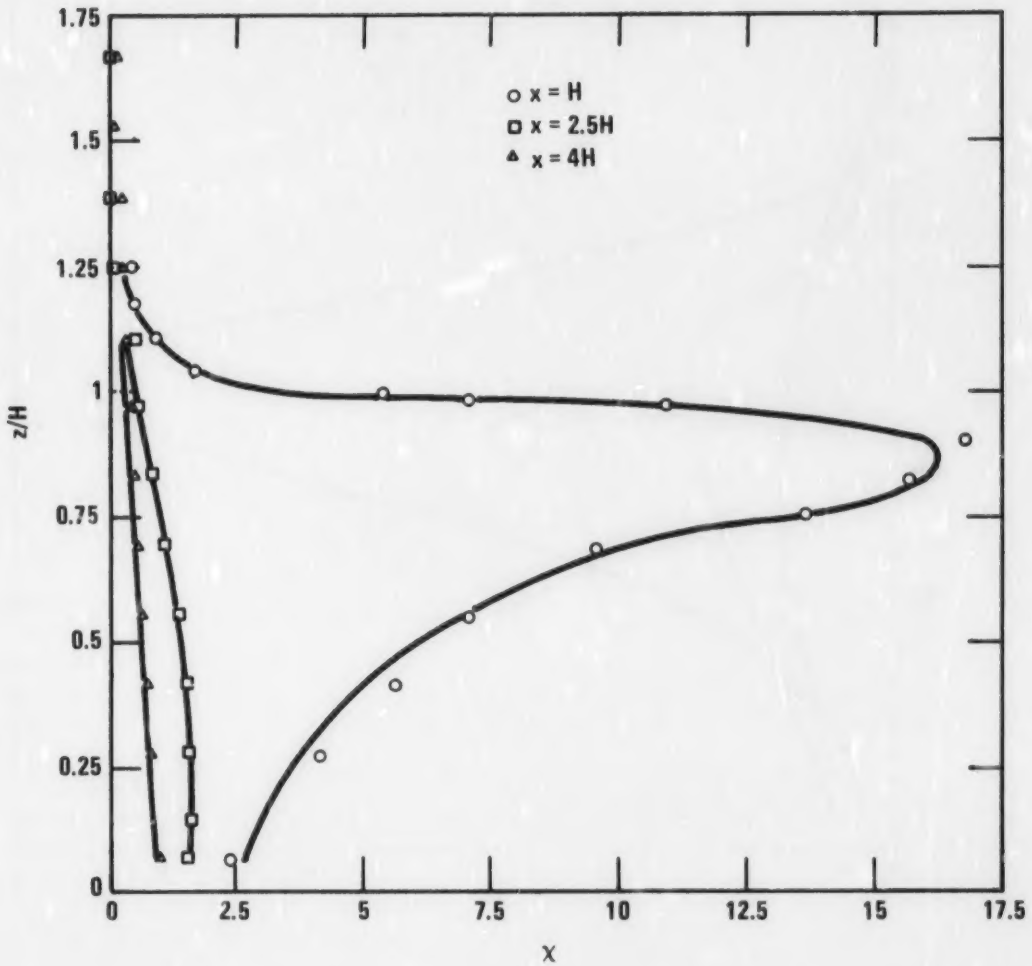

Figure 24. Vertical concentration profiles for Case 6. (y = 0.)

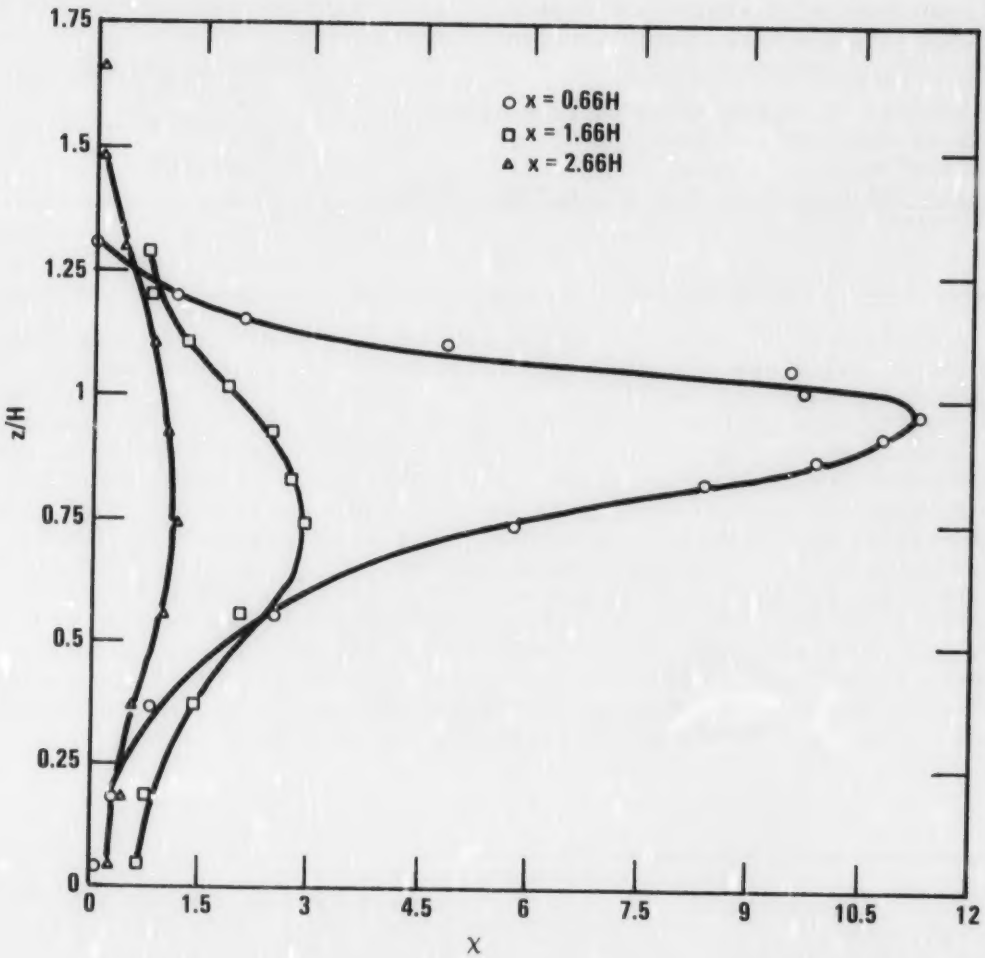

Figure 25. Vertical concentration profiles for Case 7. (y = 0.)